CONF-8809317--1

INDUSTRIAL APPLICATIONS OF NEUTRON DIFFRACTION*
(Invited Talk)

G. P. Felcher
Materials Science Division
Argonne National Laboratory
Argonne, Illinois 60439

January 1989

CONF-8809317--1

DE89 009869

International Symposium on the Industrial Applications
of the Mossbauer Effect
Parma, Italy, September 12-16, 1988
To be published in a special issue of Hyperfine Interactions

---

*Work supported by the U.S. Department of Energy, BES-Materials Sciences, under contract #W-31-109-ENG-38.

INDUSTRIAL APPLICATIONS OF NEUTRON DIFFRACTION

G.P. Felcher

Argonne National Laboratory, Argonne IL 60439

Neutron diffraction (or, to be more general, neutron scattering) is a most versatile and universal tool, which has been widely employed to probe the structure, the dynamics and the magnetism of condensed matter. Traditionally used for fundamental research in solid state physics, this technique more recently has been applied to problems of immediate industrial interest, as illustrated in examples covering the main fields of endeavour.

1. Introduction

What is neutron diffraction? Slow neutrons have an associated wavelength and thus are diffracted in the same way as light by objects, which are "rough" or inhomogeneous over a distance comparable to the wavelength. Since this is customarily of the order of the atomic spacing in condensed matter, neutron diffraction explores the atomic structure, or the spatial correlation of an atom with his immediate and more distant neighbors. This information is certainly collateral to that obtained in a resonance experiment as primarily is the Mössbauer effect. Purpose of the present communication is to show the basic phenomenology of neutron scattering and to illustrate its industrial applications with some example rather than attempting a systematic treatise that the concerned reader may find in the literature [1-3].

2. Bragg's law

Consider a plane wave of neutrons, of wavelength λ and frequency ν, travelling from left to right as depicted in Fig.1. The bars indicate the fronts of equal phase for the wave

$$\psi = A \exp[2\pi i(x/\lambda - \nu t)] \qquad (1)$$

The wave fronts are displaced by $\Delta x = \lambda$. An atom in the wave's path generates a secondary, spherical wave which is centered on the atom and has an amplitude

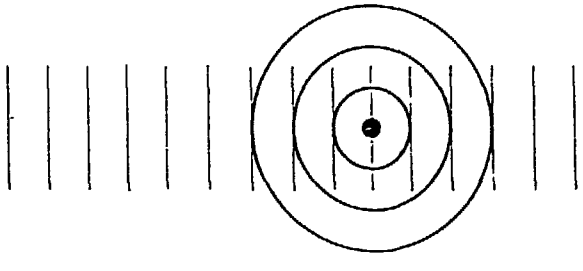

Fig.1. Scattering of a neutron from a single, pointform center.

dependent on the nature of the scattering center. A convenient way to represent this wave is by drawing the fronts of equal phase.

Fig.2 shows at the left the scattering from a row of five equal atoms. The scattered waves give now a resultant with an amplitude dependent on the direction, in which the observation is made. The resultant wave is easily obtained by joining with lines the wavefronts of equal phase of the individual waves emitted by each atom. If instead of atoms we have lines of atoms, as shown at the right side of Fig.2, the condition for having an interference maximum is simply expressed by:

$$2 \sin\theta/\lambda = 1/d \qquad (2)$$

where d is the spacing between the atomic planes, λ the neutron's wavelength.and θ is the angle formed by either the incident or the diffracted beam with the atomic planes. This relation, which is called Bragg's law, is the basis for the comprehensive description of all scattering phenomena. Reviewing a few of the pertinent points, it is clear that the maximum of the diffracted intensity becomes sharper (i.e., better defined in angle) for an increasing number of ordered atoms. A three-dimensional lattice of atoms (a single crystal) does not diffract neutrons of a given wavelength unless is oriented properly compared to the incoming beam.

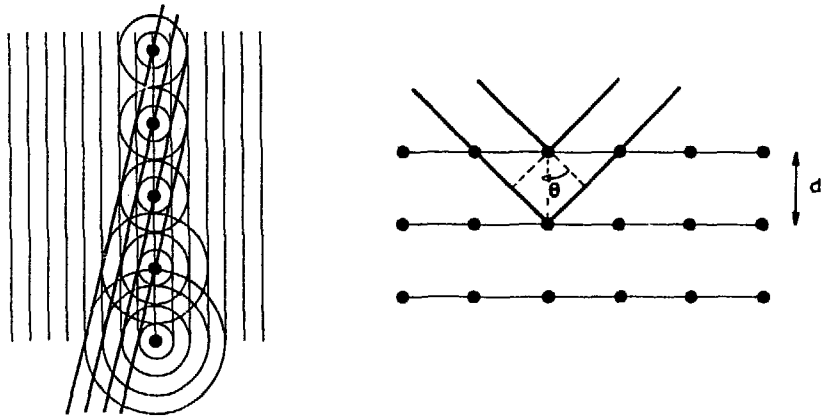

Fig.2. Left: the neutron wave travelling from left to right is scattered by a row of atoms. The resultant scattered wave has almost planar form. Right: incoming and diffracted waves from a row of planes, each containing many atoms.

The Bragg's law, as written in Eq.(2), is too restrictive. Just by observing Fig.2 (left) it is clear that a second direction for an interference maximum is obtained by joining the wavefronts of adjacent atoms which differ by two (rather than one) wavelengths. In other words, in Eq.(2) λ may be substituted by $n\lambda$, where n is any running integer, positive or zero. The case n=0 might seem trivial, because the scattered wave becomes coincident with the incoming wave, and it might be argued that the two are not distinguishable. Yet, it is important to remember that the Bragg law gives the position of the maxima, and diffracted intensity is in general occurring in a finite cone of directions

around this maximum. The maximum at the origin occurs irrespective of the distance between the atoms; as a matter of fact it takes place even for a single body of finite size. In contrast, the Bragg reflections for n>0 are present if there is at least one repeat distance d. Notice that the larger is the Bragg's angle θ, the smaller is the repeat distance: for this reason the observations of scattering are made in a space which is said to be reciprocal of the real space.

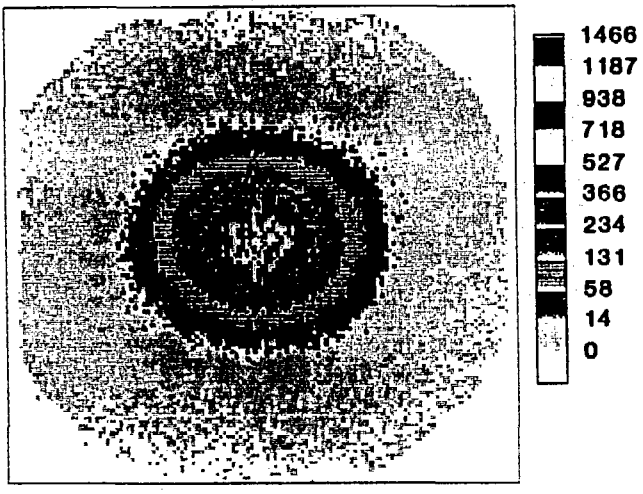

Fig.3. Small angle scattering from voids in irradiated aluminum [4]. The geometrical projection of the sample is smaller than the innermost intensity contour; the width of the "halo" indicates that the average diameter of the voids is 300 Å.

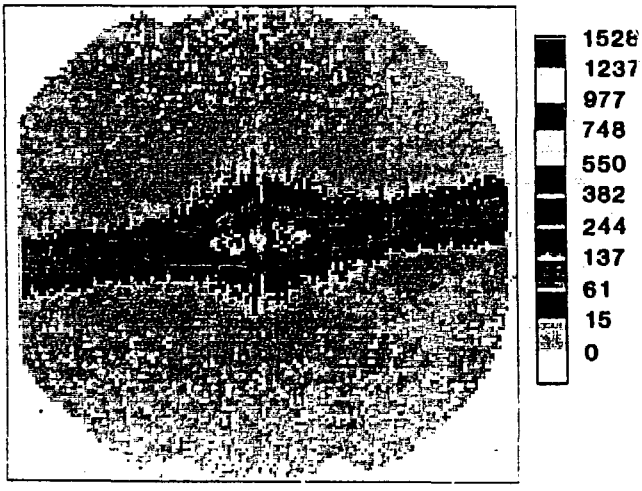

Fig.4. Anisotropic scattering pattern from a stretched poylethylene sample [4]. The individual molecular chains in the sample are very long and highly aligned; thus measurable scattering can be seen only perpendicular to the direction of stretch.

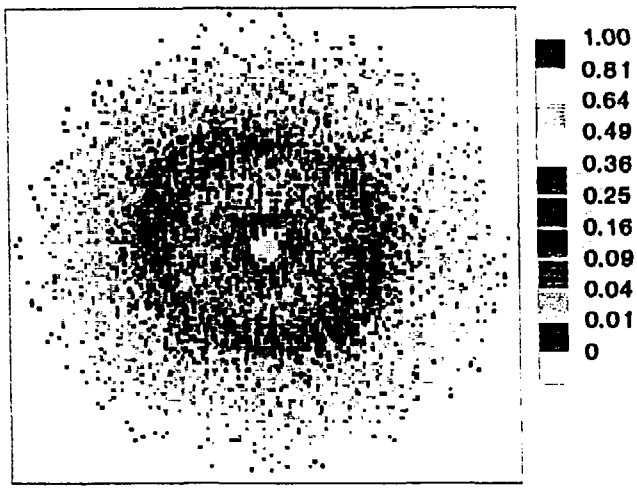

Fig.5. Small angle scattering from a block copolymer [4]. The diffraction ring is evidence that the block copolymer has an internal structure, with a head to tail distance of 700 Å.

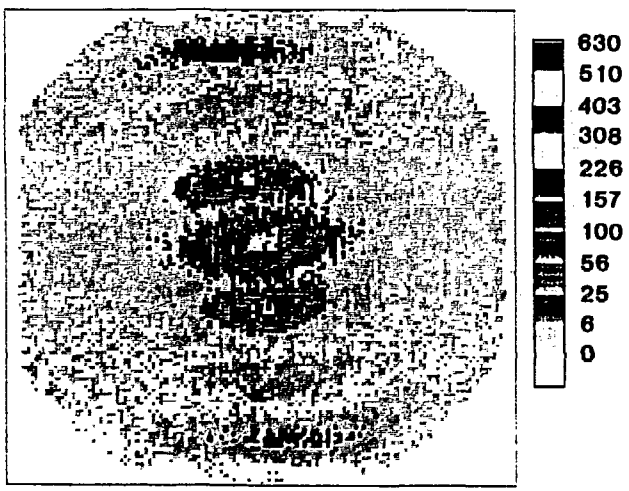

Fig.6. The one-dimensional diffraction pattern from fibers of Kangaroo-tail collagen [4]. The (uniform) spacing of the collagen molecules, which gives rise to the diffraction pattern, is of 650 Å.

The considerations made above are illustrated with a few examples of increasing complexity [4]. Fig.3 shows the scattering from independent voids caused by irradiation. Fig.4 shows an example of anisotropic scattering, caused

by stretched polyethylene. In Fig.5 the presence of a diffraction ring gives evidence that block copolymers have an internal structure. For a fiber (as the kangaroo-tail collagen of Fig.6) there is a highly correlated structure but only along one direction.

After describing the geometry of the scattering process, it is worthwhile to examine why the neutrons are scattered from single atoms in first place. The most important and universal interaction is between the neutron and the nucleus; this interaction is characterized by a length, the scattering amplitude b, which roughly speaking has the diameter of the nucleus. This is just a very minute fraction (10^{-4}) of the atomic radius, which means that a slow neutron has only a slight chance of interacting with the nuclei in a material. The weakness of the neutron/matter interaction has on one hand permitted the exploration of materials even well below their surface and in the bulk, but on the other hand has prevented fast data collection -- this difficulty being compounded by the relativlly weak intensities of the present day sources.

Roughly speaking, the scattering amplitude varies vary gradually with the atomic number; however nuclear resonances may have a deep effect on the relative scattering amplitudes of the nuclei of adjacent elements and even of isotopes of the same elements [5]. One of the fundamental advantages of neutron scattering is the possibility of "coloring" chemically identical substances by selective isotopic replacement: particularly effective has been the substitution of light with heavy hydrogen in studies concerning organic substances. Neutrons interact also with the magnetic fields encountered in their path in the materials, because neutrons carry a magnetic moment. The strength, and even the sign of this interaction depends on the relative orientation of the neutron's moment and the magnetic field. In strongly magnetic material) the magnetic scattering can be of the same order of magnitude as that due to the nuclear interactions.

3. Neutron sources

Neutrons for research are produced in large machines, available only at a few nuclear centers. The neutrons are produced either as a result of a self-sustaining fission process (as in a nuclear reactor) or by spallation. In Figs. 7, 8 is presented the scheme of one of these facilities: as the scale indicates, this is not a small operation. In this case the neutrons are produced by "spallation", as it is called the process by which an energetic proton beam hits a target and this "evaporates" neutrons [6].

Fig.7 shows how the proton beam is accelerated, while Fig.8 gives a detailed view of the spallation target: this is made of a heavy element, like tungsten or uranium, whose nuclei are rich in neutrons. The evaporated neutrons are fast - with energies of a few millions of electronVolts - and they need to be slowed down or thermalized by suitable moderators surrounding the target. The entire process, from the spallation to the cooling of the neutrons, takes place in a few microseconds. Most of the accelerators operate in the pulsed mode, and as a consequence the neutron source is pulsed. In contrast, the nuclear reactors are steady state sources of neutrons. The source feeds a number of instrument, each individually attuned to a particular kind of experiment. Their design depends in part on the nature of the sample used (which could be,in progressive degree of order, liquid, glassy, polycrystalline or single crystal) ; in part it depends on the type and the complexity of the information that is being sought. It is fortunate that the neutron sources emit neutrons with a broad spectrum of energies (and wavelengths) from which can be selected the most appropriate band for virtually any kind of problem. The samples can be set with relative ease in extremes environments, such as low temperatures (0.001 K), high temperatures (1000 C) or high pressures (30 kilobars): many structural materials provide windows which are (even if fairly thick) transparent to neutrons.

The applications of the technique have been numerous [7]. Diffraction from polycrystalline ingots under stress or pressure gives detailed information on

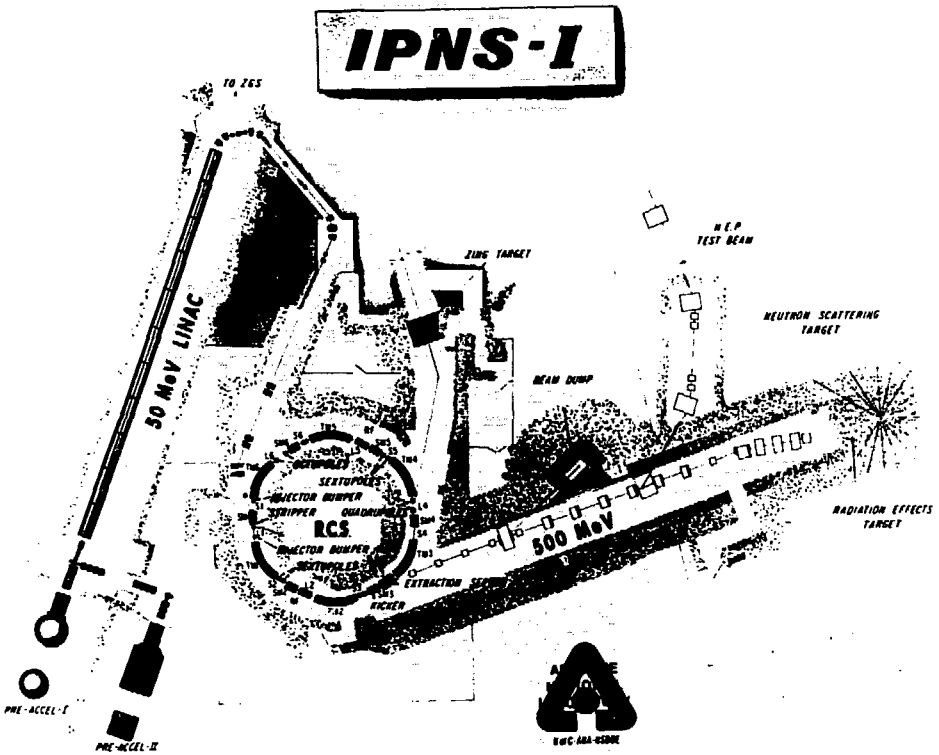

Fig.7. The Intense Pulsed Neutron Source at Argonne National Laboratory. A beam of H^- particles is accelerated to 50 MeV in the LINAC at the left; the hydrogen ions are then stripped of their electrons upon entering the Rapid Cycling Synchrotron, which accelerates the protons to 500 MeV. This proton beam hits the neutron conversion target.

the size and direction of the microscopic strain thus induced (for instances, large stresses are created as a consequence of welding). Crystalline structures are determined including the positions of those light atoms that have an important function (hydrogen atoms in organic materials; oxygen positions in superconducting oxides). Small angle scattering of cold neutrons is widely used to examine non-homogeneous systems determining the size of the aggregates (in the range of 10-1000 Ångstroms), their shape and correlation of the different phases. This technique is utilized to solve problems of metallurgy , for instance assessing the presence of copper clusters in recycled steel; as an aid to the chemical processing of coals and shales, by assessing the number and size of voids; in biochemistry, in measuring the radius of gyration of organic materials in solution. Additional applications of neutron scattering are in the field of magnetism and in the spectroscopy of light atoms, notably hydrogen. Here a detailed description will be given for only a few examples of industrial applications. A companion article of this conference deals with the metallurgical applications of small angle scattering [8].

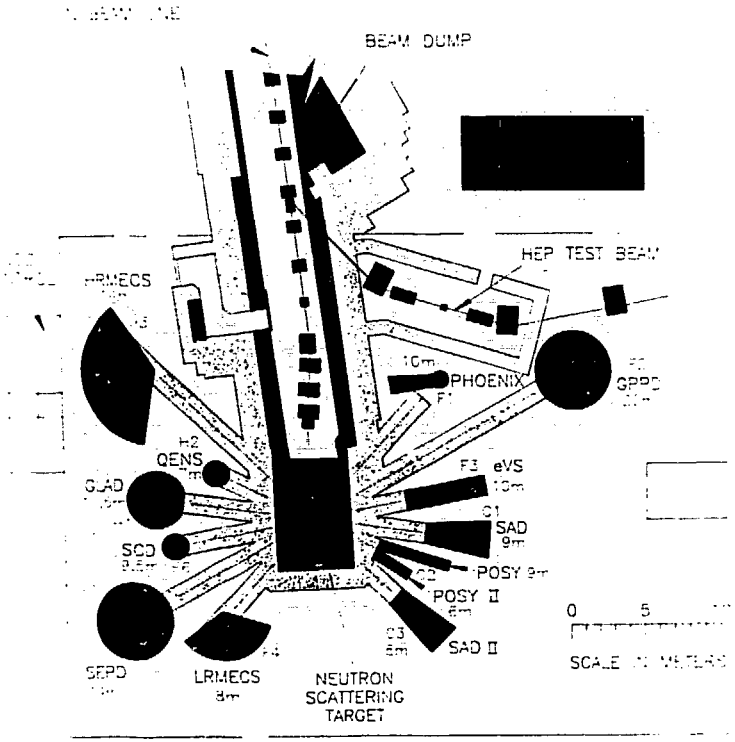

Fig.8. Detail of the uranium conversion target at I.P.N.S. The target is surrounded by hydrogenous material (moderator) whose function is to slow down the neutrons. This is in turn surrounded by a thick biological shield. Of the instruments shown in the figure, three are for diffraction studies on polycrystalline samples, one for single crystal, five for studying excitations in solid and liquids, two for small angle scattering and two for neutron reflection.

4. Metallurgy: residual stresses

When first formed, components such as welds contain internal stresses of magnitude up to a large fraction of the yield stress. These have great importance since any extra applied stress may lead to deformation and fracture. The most frequently used technique for the determination of internal stress involves strain gauges: the changes in strain are measured as part of the material is drilled or machined away. The technique is simple, but is destructive and lengthy. Ultrasonic methods offer a better chance of a portable stress measuring device. However they measure only an average stress along the flight path and require careful corrections for the effect of texture. X rays have been used for many years for measuring stresses, but only for near-surfaces, where stresses are necessarily different from the bulk. High-resolution neutron diffraction is the only non-destructive method available for

measuring the full internal stress tensor within a bulk component. Here some results will be shown on the measurement of the internal stresses in deformed, polycrystalline Zircaloy-2, a material widely used for cladding of the uranium rods in a nuclear reactor [9].

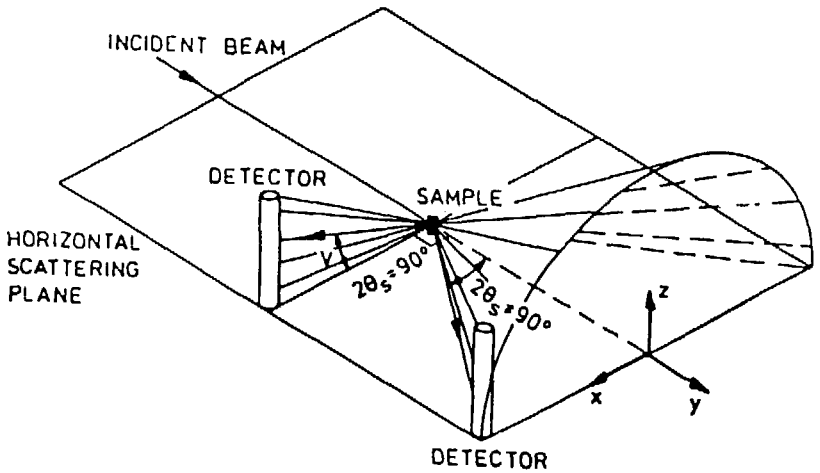

Fig.9. The geometry of scattering for a polycrystalline sample. All the directions on a cone at an angle 2θ with the incident beam are equivalent. A single detector (which usually has the shape of a long cylinder) is placed in a satisfactory geometry when it follows a segment of this cone.

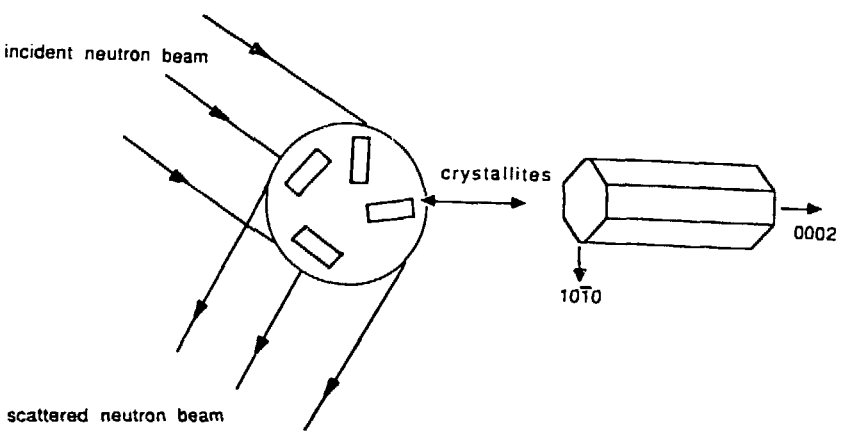

Fig.10. View from the top of the sample. Of all the grains composing the sample only some have the orientation necessary to diffract neutrons along a given direction. The crystalline form of Zircaloy-2 is put in evidence for one of the grains.

The instrument used is a "powder" diffractometer, whose working at a pulsed neutron source is sketched in Fig.9. The sample scatters the neutron beam all around, and the intensity of the scattered radiation is measured by detectors, placed at calibrated angles with the initial beam. Since the source is pulsed, the distance source-sample-detector is travelled by neutrons of different wavelengths in different times; hence the wavelength of the detected neutron is defined by the time of flight [10].

The sample is a polycrystalline rod (usually with a volume of a few cubic centimeters): the crystal grains, separated by dislocations, point in all directions as sketched in Fig.10. However, the Bragg's law selects the diffracting grains for each wavelength on the basis of their orientation. A characteristic diffraction pattern of Zircaloy-2 is shown in Fig. 11. The labels on the peaks are the Miller indices [5] for the hexagonal Zircaloy-2 crystal structure; they correspond to sequences of planes along different orientations of the crystal, and thus expected to have different physical and mechanical properties. For instance, as shown in Fig.10, the $(10\bar{1}0)$ planes form a sequence in the basal plane of the hexagon; the (0002) sequence is along the hexagonal axis. One rod was subjected to tension well above the limit for plastic deformation, and then the stress was released. A second, identical rod was subjected to a similar procedure but compressing the rod.

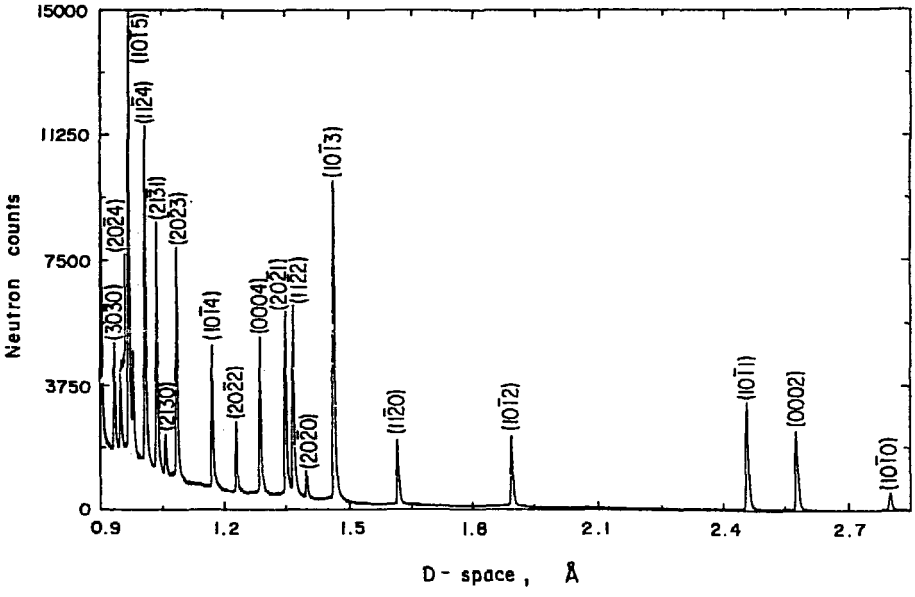

Fig.11. Part of the diffraction pattern obtained for Zircaloy-2 in a bank of detectors. The abscissa is $(2\sin\theta/\lambda)^{-1}$; when this corresponds to the spacing of a Bragg reflection, the relative label is given.

The effect of the residual stresses on the interatomic spacings can be appreciated by looking at single Bragg reflections. As it can be seen in Fig.12

the residual stresses along two mutually perpendicular crystallographic orientations are opposite. Variations of the interatomic spacing as small as 0.3 parts in a thousand are well observable; and from the shift of an adequate number of Bragg reflection is possible to reconstruct the full distortion of the atomic configuration which takes place in the crystalline grains after stressing the material.

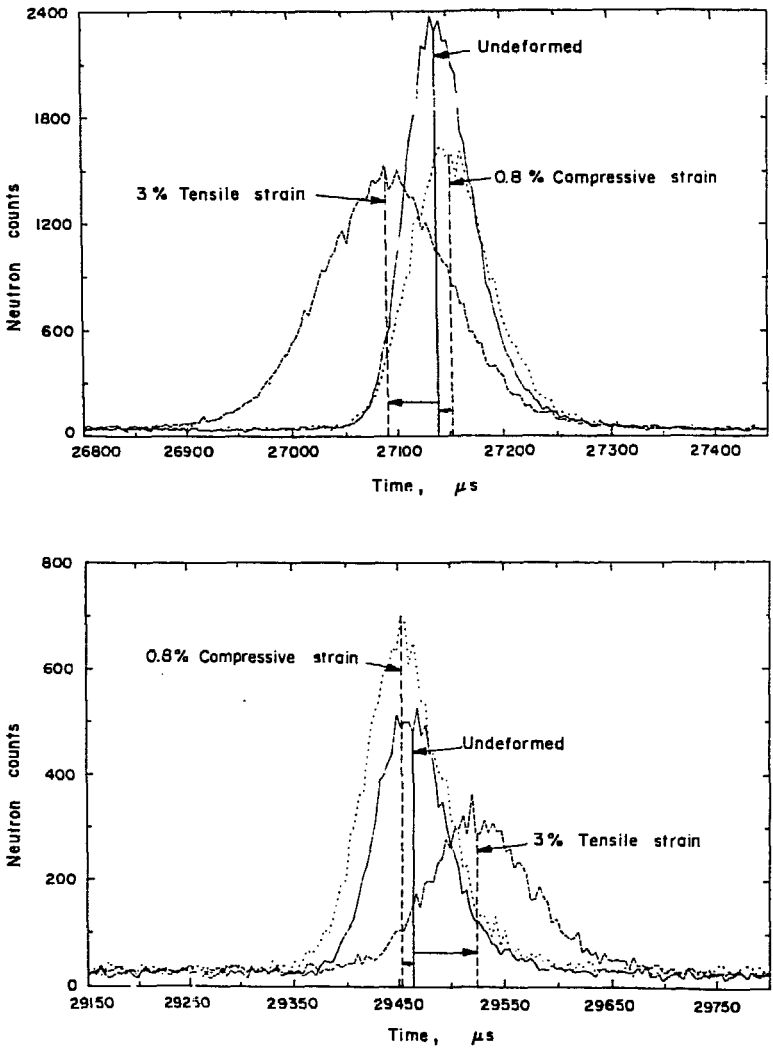

Fig.12. The effect of the plastic deformation on the position and shape of the (0002) line (top) and the (10$\bar{1}$0) line (bottom) of Zircaloy-2. The abscissa gives the time of travel of the neutron from the source to the detector.

5. Catalysis: the working of the zeolites

The motion of molecules in the pores of molecular sieve zeolites is of considerable interest, because zeolite catalysts are widely used in industry.

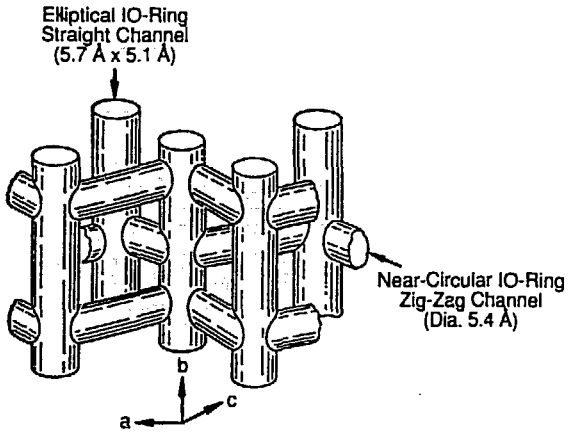

Fig.13. Diagram of the channel structure of ZSM-5 zeolite.

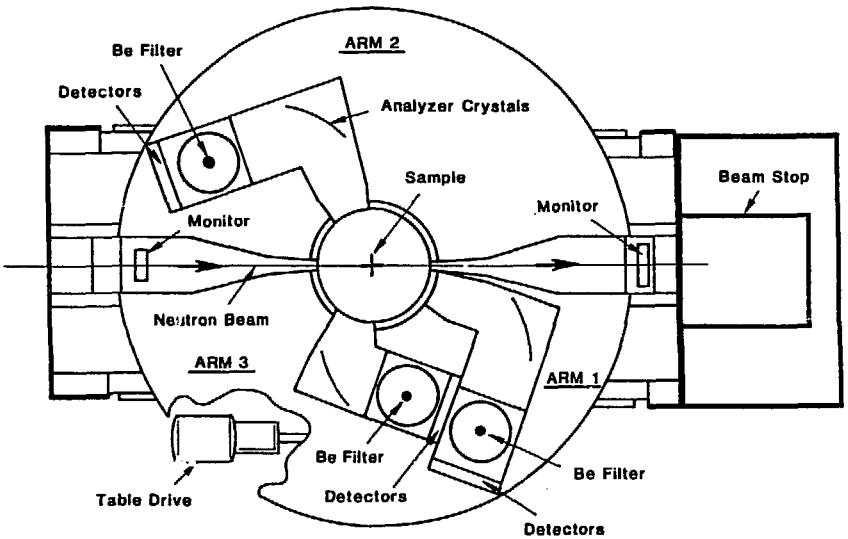

Fig.14. Schematic diagram of the Quasi Elastic Neutron Spectrometer. Three analyzing arms, each containing analyzing crystals, low energy passing beryllium filters and detectors, cover different portions of the scattering space.

In zeolites hydrocarbons react selectively, depending on their molecular shape: this is a consequence of the unique combination of the catalytic sites present on the internal surface of the zeolite and the molecular sieving effects of the pore network. Thus it is interesting to inquire how readily a molecule can diffuse in a network, such as that shown in Fig.13; secondly, how the chemical bonds of the molecule are affected by the presence of the cage.

Neutrons provide an excellent probe of the motion of hydrocarbons in zeolites for a sum of fortunate circumstances. First of all, the zeolite cages, made of silica or alumina, are practically transparent to neutrons. In contrast, the cross section of the hydrogen nuclei in the hydrocarbons is the largest for all elements [11]. The neutron scattering process takes place while the molecule is in motion: hence the energy of the scattered neutron is "Doppler shifted" from its initial value. This variation of the energy is measured in a neutron scattering instrument, where an extra leg has been added to analyze the wavelength - and the energy - of the scattered neutrons (see Fig.14). In pilot experiments [12] on the most simple of the hydrocarbons, methane, in the channel structure ZSM-5 zeolite of Fig.13, an energy broadening of the neutron line has been found of the order of 100 microelectrovolts, corresponding to a diffusion constant (at room temperature) of 5×10^{-5} $cm^2 s^{-1}$.

The neutrons are capable of exchanging energy with the molecule, and thus the full spectrum of the scattered neutron provides a picture of the excitation spectrum of the molecule reminiscent of the Raman spectrum obtained with infrared radiation. The spectrum becomes the richer, the larger is the molecule.

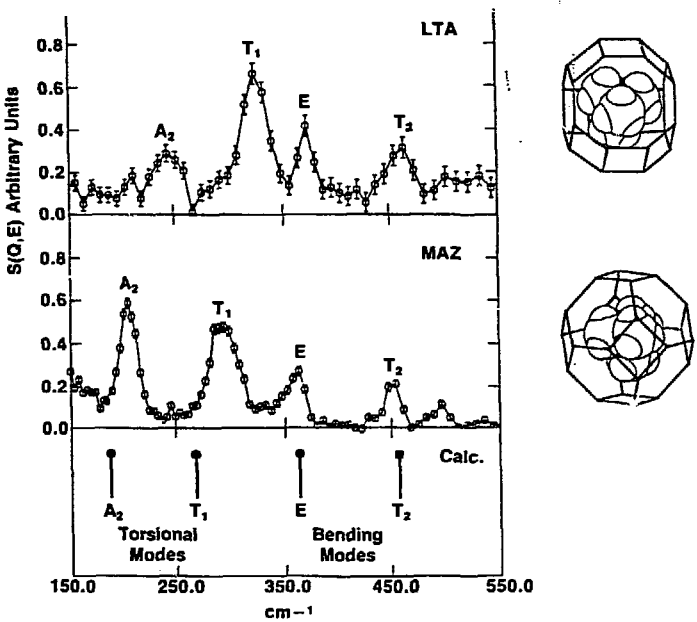

Fig.15. The torsional and bending modes of tetramethylammonium, in cages of MAZ and LTA zeolites. The relative cages are drawn on the right side of the figure; the TMA molecule is more constrained in the smaller LTA cage.

For instance in Fig.15 is shown [13] the spectroscopy of the hydrogen in tetramethylammonium (TMA) hydroxide in the zeolites omega (MAZ) and ZK-4 (LTA). In contrast with that of Fig.13, in these zeolites the cage is larger than the entrance. The size of the cage affects the spectrum of the intramolecular excitations, and particularly those of lowest energy, as the torsional modes and the bending modes of the CH_3 groups. When in a larger cage, as in MAZ, these modes have energies indistinguishable from those of the free molecule; while in the smaller LTA zeolite cage the motions are hindered, with a stiffening of the energies which is particularly evident for the torsional modes.

6. Magnetic tapes

Sputtered films of iron oxides form a widely used class of recording materials for high-density recording media. They may be prepared in many ways: for instance films of Fe_3O_4 are prepared by reactive sputtering of an iron target in an argon-oxygen plasma; these films can be transformed into the γ-phase of Fe_2O_3 by oxidation in air at elevated temperature. For the purpose of better impressing and retaining a magnetic memory is important that the film has a high coercive field and that the hysteresis loop (Fig.16) is square with a susceptibility at saturation as low as possible. These conditions are more closely achieved when the Fe_3O_4 film is roasted and oxidized to the γ-Fe_2O_3 state.

A question which had beene long unansvered is: how uniform is the magnetization throughout the film? Unfortunately, the thickness of these films (typically a fraction of a micron) makes conventional probes of their magnetic profiles inadequate. For example, spin polarized photoemission is sensitive to the topmost layers only and while depth profiling is possible it is only with physical removal of subsequent layers of the film. A second technique, the magneto-optic Kerr effect, probes deeper into the film but gives only a qualitative (yes or no) answer. Yet the problem was easily solved by means of polarized neutron reflection [14].

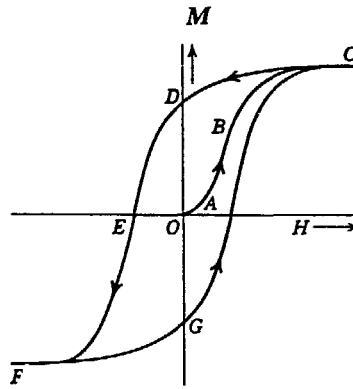

Fig.16. The magnetization M of a ferromagnet as a function of the applied magnetic field H. OAB gives the virgin magnetization, while CDEFGC is the hysteresis loop. The coercive field is the length OE, which for Fe_3O_4 films is 600 Oe. OD is the remanent magnetization, which for a good magnet should be as close as possible to the saturation value.

Here the word "reflection" is by no means used figuratively: as seen in Fig.17, the reflected beam direction is entirely defined by the surface. Below the surface, we assume that the neutron interaction potential V(z) depends only

on the depth z from the surface. The propagation of the neutron waves is similar to the propagation of light in a material with graded refractive index, and is described by the Schrödinger equation along the z-axis:

$$f''_{\pm} + [k_0^2 - 4\pi(bN \pm cB)]\, f_{\pm} = 0 \qquad (3)$$

where $k_0 = 2\pi(\sin\theta/\lambda)$ is the component of the momentum of the neutron perpendicular to the surface of the reflecting body, and c is a constant. The interaction potential is formed of two parts: the first is due to the interaction with the nuclei, characterized by the scattering amplitudes b with particle density N; the second is the interaction with the magnetic field B present at the depth z from the surface. The neutron is birefringent, in the sense that the f_+, f_- are the wavefunctions for neutrons having a magnetic moment which is polarized either parallel (+) or opposite (-) to the magnetic field. For each of the two spin states, the second order Schrödinger equation can always be solved, and the wavefunction fully determined once added boundary conditions. These specify that the number of neutrons and their flux are conserved at each and every boundary.

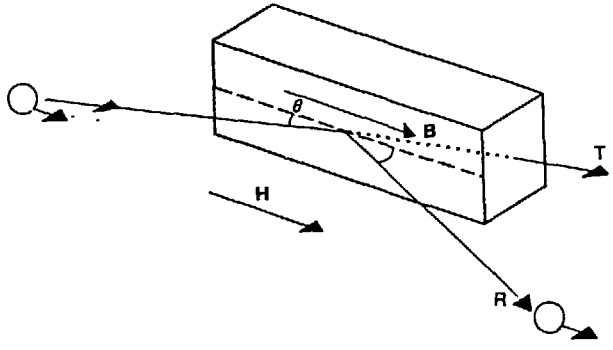

Fig.17. Scheme of a neutron reflection experiment. The angles of incidence are usually of the order of one degree. Part of the beam is reflected (R), part is refracted (T). Here the sample is magnetized along the surface, and the neutrons are polarized parallel to the magnetic field. In a typical experiment this geometry is rapidly alternated to one, in which the neutrons are polarized opposite to the magnetic field.

The wavefunction in the vacuum is given by:

$$\psi_{\pm} = \exp(ik_0 z) + R_{\pm}\exp(-ik_0 z) \qquad (4)$$

and thus is composed of an incoming and a reflected wave, whose coefficient is the reflectance. In the material instead the momentum of the neutron wave is modified to:

$$k_{i\pm} = \sqrt{k_0^2 - 4\pi(bN \pm cB)} \qquad (5)$$

For a given angle of incidence θ the neutron momentum in the material, k_i, becomes smaller the longer is its wavelength λ, until k_i becomes complex. At

this point the neutron wave no longer penetrates the material, and the beam is totally reflected. Using an experimental arrangement functioning precisely in this way (fixed angle of incidence/variable wavelength) the spin-dependent reflectivities were measured for a layer of iron oxide on silicon before and after oxidation. The results are presented in Fig.18. The samples were kept in a magnetic field (parallel to the surface) sufficient to saturate its magnetization.

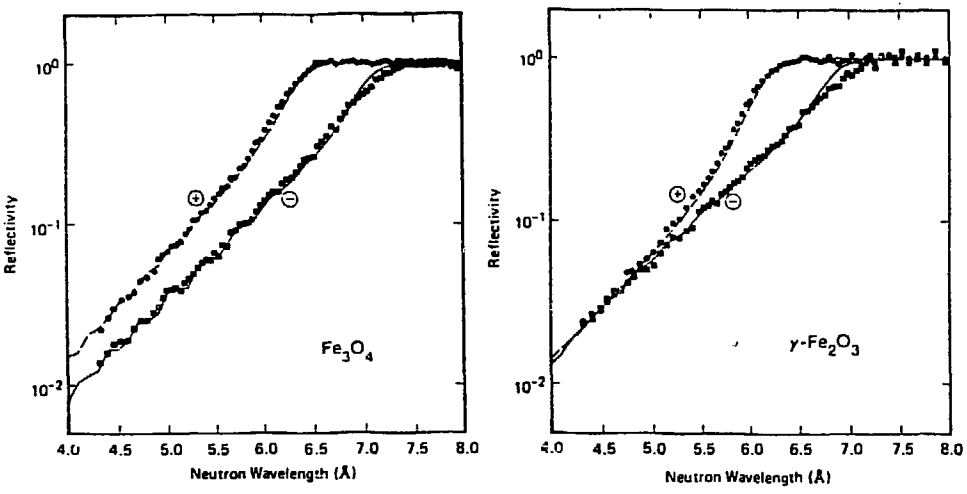

Fig.18. Reflectivities of Fe_3O_4 and its oxidized form, γ-Fe_2O_3. The reflectivities are spin dependent, for neutrons polarized along (+) and opposite (-) to the sample's magnetization. The reflectivities were measured as a function of the neutron wavelength for an angle of incidence θ = 0.55 degrees. The two lines represent the reflectivities calculated for the profiles shown in Fig.19.

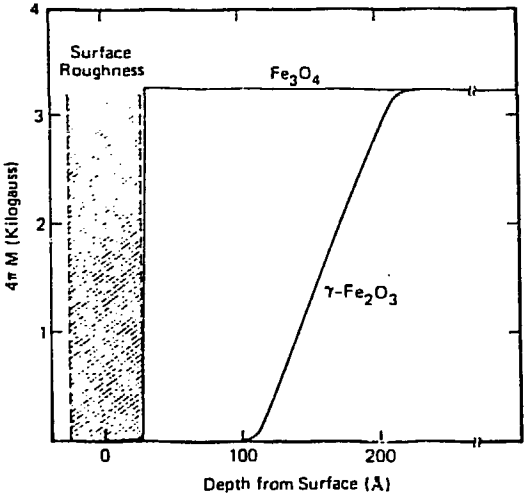

Fig.19. Magnetic depth profiles for films of Fe_3O_4 and γ-Fe_2O_3 used to calculate the curves shown in Fig.18. The dashed region corresponds to the surface roughness of the film.

The reflectivity curves show a sizeable spin dependence before as well as after the heat treatment; their striking difference immediately suggests that the magnetic profiles of the two samples are different. For Fe_3O_4, $R^+(\lambda)$ and $R^-(\lambda)$ are similar and can be almost superimposed by a proper scaling of λ. Inspection of Eq.(3) shows that this is possible when the nuclear and the magnetic scattering amplitude are constant throughout the film. As an added conclusion, the magnetization of γ-Fe_2O_3 is not uniform; and detailed profile is obtained by calculating back the potential from the reflectivity. Good fitting with the experimental data was obtained with the model profiles of Fig. 19, according to which, the process of oxidation of the sample has caused the surface to become magnetically passive for a thickness of 150 Å.

As a follow-up of this experiment, considerable work has taken place to explain why the heat-treated surface is not ferromagnetic, and to attempt to reduce this dead layer (which of course reduces the sensitivity of this material in a magnetic tape) either by modifying the thermal treatment or by chemical doping.

7. Conclusions

Neutron scattering is being used for an increasing amount of industrial applications, which at present account for roughly one quarter of the activity at nuclear centers, such as those of Grenoble and Rutherford in Europe, and Brookhaven and Argonne in the United States.

Acknowledgments

The present paper was written under the auspices of the U.S. Department of Energy,under contract W31-109-ENG-38. The author would like to acknowledge the help of the following colleagues: F. Trouw, T. Brun, L. Iton, J. Jorgensen, J. Faber, D. Kupperman, A. Mansour, A. Karim, P. Seeger and R. Hjelm Jr. To all of them my sincere thanks.

References

[1] G. Bacon, Neutron Diffraction, Oxford 1962
[2] W. Marshall and S. Lovesey, Theory of Thermal Neutron Scattering, Oxford 1971
[3] Neutron Scattering, D. Price and K. Sköld eds., Academic Press, New York 1984
[4] P. Seeger, R. Hjelm and M. Nutter,Los Alamos Report LA-UR-88-591
[5] International Tables for X-Ray Crystsllography, J. Ibers and W. Hamilton eds., Kynoch Press, Birmingham 1974
[6] J. Carpenter and W. Yelon, in reference [3]
[7] M. Hutchings and C. Windsor, in reference [3]
[8] G. Kostorz, International Symposium on the Industrial Application of the Mössbauer Effect, Parma (Italy), September 1988
[9] S. MacEwen, J. Faber Jr and A. Turner, Acta Metall. 31, 657 (1983)
[10] C. Windsor, Pulsed Neutron Scattering. Taylor and Francis, London, 1981
[11] The scattering is referred to here is incoherent. For a comprehensive discussion of the coherent and incoherent scattering, see reference [1].
[12] IPNS Progress Report, Argonne National Laboratory, 1988 (unpublished).
[13] T. Brun, L. Curtiss, L. Iton and R. Kleb, J. Am. Phys. Soc. 109, 4118 (1987).
[14] S. Parkin, R. Sigsbee, R. Felici and G. Felcher, Appl. Phys. Lett. 48, 604 (1986).